Advances in Colloid and Interface Science, 39 (1992) 61–75
Elsevier Science Publishers B.V., Amsterdam

HYDRODYNAMIC FINGERING INSTABILITY OF DRIVEN WETTING FILMS

A.M. CAZABAT**, F. HESLOT, P. CARLES, S.M. TROIAN*

Collège de France

Physique de la Matière Condensée

11, place Marcelin Berthelot

75231 PARIS CEDEX 05

FRANCE

Introduction

The spontaneous spreading of thin wetting films under capillary forces alone is typically a slow process. The application of a surface stress can drive the spreading more quickly : for instance, temperature gradients induce surface tension gradients along the film surface, pulling the liquid towards the high surface tension regions.

Let us consider a flat film (xy plane) of constant thickness h_o, in the absence of gravity and let us impose a surface tension gradient $\tau = \frac{d\gamma}{dx}$ along x. A Couette flow in the x direction results, the average velocity V of which is

$$V = \frac{h_o \tau}{2\eta}$$

---

* Permanent address : Exxon Research & Eng. Co., Clinton twp. - Route 22 E, Annandale, N.J. 08801, USA.

** Person to whom correspondence should be mailed.

0001-8686/92/$15.00

Here, η is the fluid viscosity.

In practical situations, more complicated flows with recirculation are observed. Very often, mixed effects of gravity and surface tension gradients cause instabilities and convection rolls, especially for relatively thick films.

The aim of the present study is to analyse the influence of a thermal surface tension gradient on thin films of completely wetting, nonvolatile liquids, in the capillary rise geometry.

The solid surface is vertical (xy plane) with x in the vertical direction and is dipping into a reservoir of liquid, the free surface of which (far from the solid) is the yz plane. Without any gradient, a quasi-equilibrium state is reached rapidly (after a few seconds for moderately viscous liquids), where the (wetting) liquid has built a meniscus of typical size $\sim$ mm tangent to the solid surface (fig 1a).

However, a microscopic observation of the meniscus edge shows that the system is not yet at equilibrium at this scale : a thin (nm) wetting film grows on top of the edge (fig 1b). For the nonvolatile liquids we study, this growth is very slow (1) and we are always very

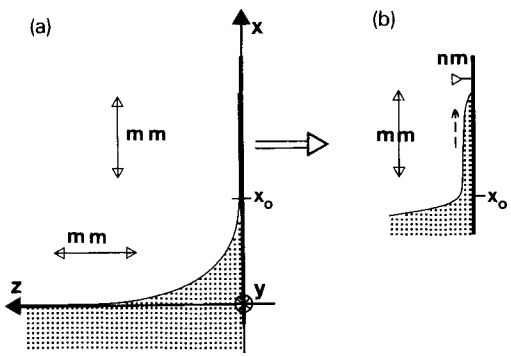

Fig.1 a • - Definition of the reference frame and shape of the meniscus at the macroscopic scale. The wafer is vertical (xy plane). The free liquid surface is horizontal (zy plane).
b • - Magnified view of the top of the meniscus. Vertical scale unchanged, magnified z-scale.

far away from the full equilibrium state, corresponding to the balance between disjoining pressure and gravity (2).

In the presence of a vertical negative temperature gradient dT/dx inducing a positive surface tension gradient $d\gamma/dx$, the wetting film becomes thicker and faster. Its behaviour depends on the gradient strength but also, in a somewhat subtle manner, on the way it is fed from the macroscopic meniscus. This will be illustrated by comparing our experiments (3) with the previous study by Ludviksson et al. (4).

I. Experimental setups and observations

1. Experimental setups (3,4)

In our case, the solid surface is a silicon wafer, covered with natural oxide, held pressed vertically against two temperature-controlled holders (fig. 2). The liquids are light silicone oils

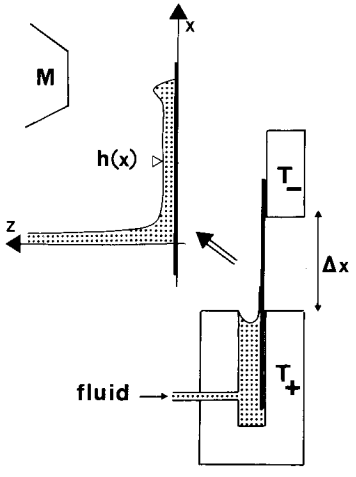

Fig.2 Schematic view of the experimental setup.
M : microscope. Upper left : magnified view of the Marangoni film.

(polydimethylsiloxanes, abbreviated as PDMS) which are nonvolatile and completely wet the solid. The viscosity η has been varied between 0.02 and 0.5 Pa.s, the surface tension being always $\gamma = 0.02\ Nm^{-1}$. The temperature dependence of the viscosity has been shown to have negligible effect on the studied phenomena. The temperature dependence of the surface tension is characterized by:

$$\frac{1}{\gamma} \cdot \frac{d\gamma}{dT} = -2.5\ 10^{-3}\ K^{-1}$$

constant in a wide range of temperatures.

The temperature gradient dT/dx is built along the wafer by imposing a temperature difference ΔT between the two holders which are Δx apart. The gradient is constant between the holders, thus $dT/dx = \Delta T / \Delta x$. Various gradients are obtained by changing Δx, ΔT being kept constant. Here, ΔT = 28°C, the upper holder is colder (T = 19°C), the lower one, which is at the level of the macroscopic meniscus, is warmer (T = 47°C).

Just at the meniscus, films are thick and the thermal pattern with the hot wall vertical is unstable.

Actually we have some hints of a convection roll existing just below the meniscus, although it has not been studied systematically. Anyway, the injection conditions at the bottom of the thin film may be largely unknown, but they are identical for all the measurements.

Numerical values of the various parameters are given in the table I, together with the ones chosen in the experiment by Ludviksson and Lightfoot (referred to as L.L.).

In this latter case, the surface tension gradients are lower. Also the injection is striklingly different, occuring not at the meniscus, but by means of a relatively thick film obtained by dipping the solid into the liquid, taking it out and letting the film drain by gravity.

TABLE I

$h_{o_{max}}$	τ (Pa)	h_o (μm)	v (μm/s)	θ_{Tanner}	θ	e_o (μm)	x_1 (mm)
81	0.5	0.86	8*	0.07	0.05	0.02	$4x10^{-4}$
52	0.27	0.65	3*	0.05	0.05	0.02	$4x10^{-4}$
40	0.21	0.54	3	0.05	0.04	0.025	$6x10^{-4}$
20	0.10	0.27	1	0.036	0.03	0.033	10^{-3}
10	0.054	0.17	0.3	0.024		0.05	$2.5x10^{-3}$
3.4	0.018	2.35	0.33	0.025	0.006	0.17	$3x10^{-2}$
2.5	0.013	1.7	0.15	0.019	0.0035	0.3	$8x10^{-2}$
1.7	0.009	1.1	0.06	0.014	0.00075	1.3	1.8

PDMS η = 0.02 Pa.s γ = 0.020 $N.m^{-1}$

SQ η = 0.021 Pa.s γ = 0.027 $N.m^{-1}$

☐ : L.L. experiment

* : linear part too short to get a precise reading (instability starts).

2. Observations

In both experiments, a flat film of thickness h_0 grows along the solid. After some time, h_0 becomes constant with time and a linear growth of the film length at constant velocity V is observed.

Nothing else occurs in the L.L. experiments; at the edge, the film thickness decreases monotonically from h_0 to 0.

In our experiment, a bump develops at the film edge. This bump soon becomes unstable and tends to break into droplets, in a sort of Rayleigh-like instability. As the thicker parts climb faster than thethinner ones, a fingering instability ultimately results.

The sequences are followed under microscope at low magnification. As the silicon wafer is reflecting, equal thickness interference fringes are easily observed and are used to reconstruct the thickness profiles. Examples of fringes patterns and corresponding profiles can be found on figures 3 and 4.

Measured values of h_0 and V (in our case, V is the velocity before the instability starts) are given in table I. The films in our

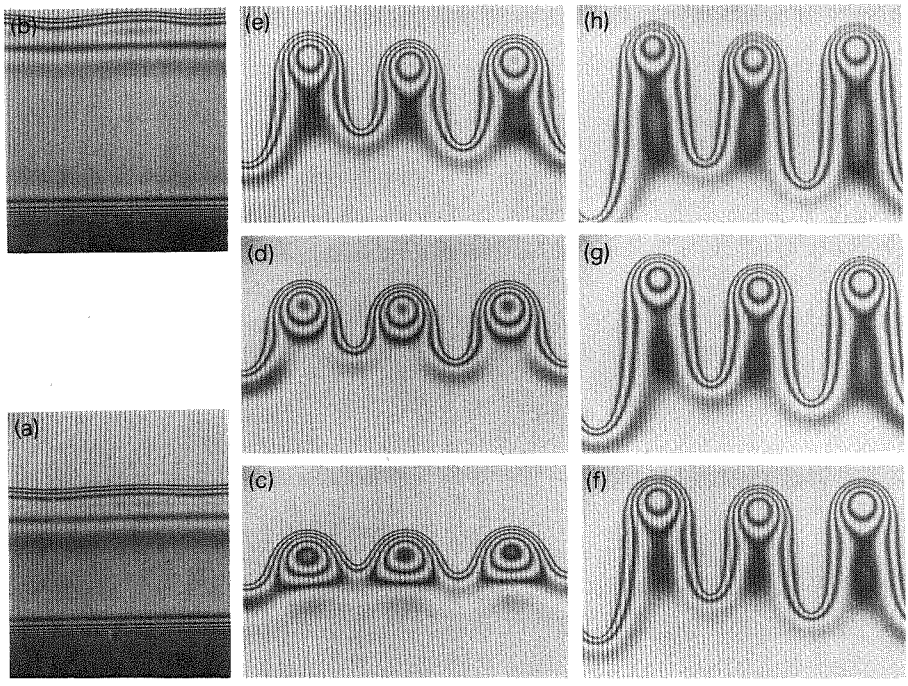

Fig.3 Photographs of equal thickness fringe patterns produced by the Marangoni film at increasing times. Plane of the photograph : xy plane, vertical axis x, horizontal axis y. (Vertical fringes are spurious interferences in the optics). Thickness spacing of the fringes : $\lambda/2n$. $\lambda = 6328$ Å (He-Ne laser) n = 1.4 (index of PDMS). In the two first photographs (a and b) the meniscus can be seen at the bottom. Later, the film is too long and the meniscus is out of the field.

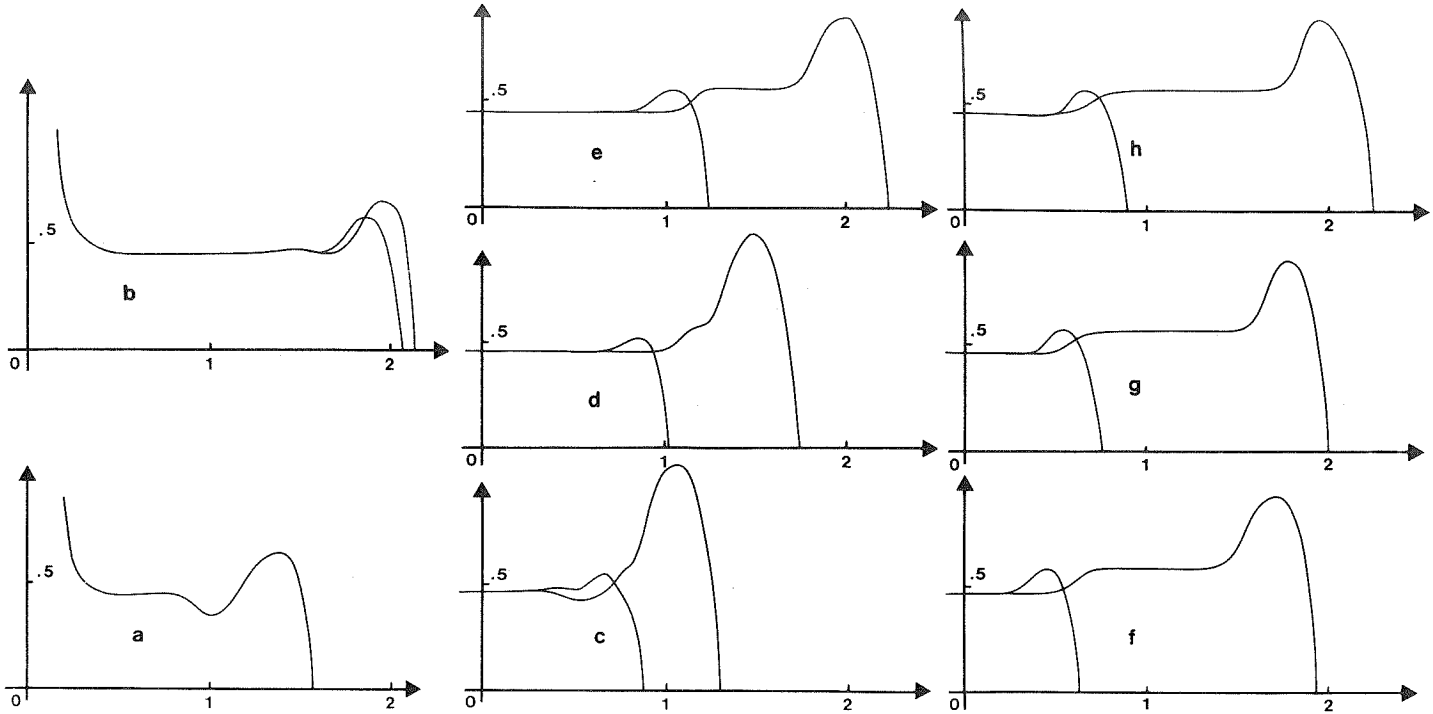

Fig.4 Thickness profiles corresponding to the previous photographs.

Vertical axis z.

Horizontal axis x (for convenience).

experiment are thinner and faster than in the L.L. experiments. A hydrodynamical description neglecting gravity accounted satisfactorily for our measured values of V (3). Here, we shall rather try to explain the striking differences between L.L. experiment and ours. So we address the problem in a general way, taking gravity into account.

II. Theoretical analysis

While "thick" films, the thickness of which is around the micrometer, are described by purely hydrodynamic equations, "thin" films are not: the equations must be supplemented by disjoining pressure terms (2). For ultrathin films, a few Å thick, molecular diffusion must also be taken into account (5).

In the present case, we can neglect molecular films, but a possible role of disjoining pressure terms at the edge of the films has to be considered. Let us start with a purely hydrodynamic analysis.

1. Hydrodynamic equations

In the stationary case, the growth of the film is controlled by the 1-dimensional Navier Stokes equation:

$$\eta \frac{\partial^2 V}{\partial z^2} = \frac{\partial p}{\partial x} + \rho g \qquad (1)$$

where V(x,z) is the fluid velocity upwards along the plate, z measures the distance from the solid, p is the pressure in the fluid and ρg the gravitational force per unit volume.

For small surface slope

$$\frac{\partial p}{\partial x} = -\gamma \frac{d^3h}{dx^3} - \frac{\partial \gamma}{\partial x}\frac{d^2h}{dx^2}$$

where h(x) defines the film surface. In the r.h.s., the second term is completely negligible compared with the first one and can be dropped. Equation (1) becomes

$$\eta \frac{\partial^2 V}{\partial z^2} = -\gamma \frac{d^3h}{dx^3} + \rho g \qquad (2)$$

Integrating equation (2) subject to the boundary conditions $V(x,z=0) = 0$ and $\eta \partial V/\partial z\ (z = h(x)) = \tau$ gives the height averaged velocity as:

$$V = \frac{h}{2\eta}\tau - \frac{h^2}{3\eta}\rho g + \gamma \frac{h^2}{3\eta}\frac{d^3h}{dx^3} \qquad (3)$$

which does not depend on x in the stationary conditions. In the flat part of the film, the last term is negligible. The velocity V becomes

$$V_F(h_o) = \frac{h_o}{2\eta}\tau - \frac{h_o^2}{3\eta}\rho g = V \qquad (4)$$

The first term describes the climbing of the film under Marangoni forces, while the second one accounts for the gravity effect.

Equation 4 shows that the thickness h_o must be less than

$$h_{o\,max} = \frac{3}{2}\frac{\tau}{\rho g}$$

in order V_F to be positive, and that the maximum value of V_F is

$$V_{max} = \frac{3}{16}\frac{\tau^2}{\rho g \eta}$$

corresponding to $h_o = 1/2\ h_{o\,max}$.

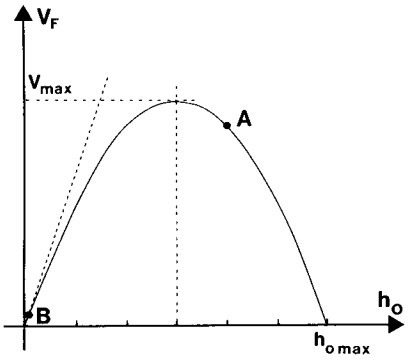

Fig.5 Velocity of the flat film as a function of its thickness h_0.

A •- : L.L. experiment.

B •- : our experiment.

Tilted dashed line : V_F without gravity.

This is illustrated on fig.5 and the corresponding values are reported in table I. In the L.L. experiment, h_0 is typically 2/3 $h_{0\,max}$, i.e. on the right of the $V(h_0)$ curve (point A). In our experiment, h_0 is about $10^{-2} h_{0max}$ (point B) i.e. in the range where gravity is negligible.

This has important consequences for the possible presence of a bump in the profile. Let us come back to equations (3) and (4) and see how the flat film of thickness h_0 will curve to contact the solid. One has

$$V_F(h) + \gamma \frac{h^2}{3\eta} \frac{d^3h}{dx^3} = V_F(h_0) \qquad (5)$$

At point A, V_F increases if h decreases. If $h < h_0$, the third derivative is negative. This is compatible with a monotonic decreasing profile tangent to the flat film, in which case all the derivatives which were zero in the flat film, take negative values. (But the argument holds only at the crossover towards the flat film). It is not so at the point B, where V_F decreases if h decreases. If h decreases equation (5) shows that the third derivative must be positive, which is

uncompatible with a monotonic decreasing profile. Oscillations will take place.

Even if this is only a part of the answer to the "bump problem", which has to be solved numerically, it is an important one. At point B, the profile cannot be monotonic. Actually, oscillations and bump are easily seen on fig.4.

At the present time, numerical calculations of the profile at point B are underway (6-7). Here, gravity is negligible. The wavelength of the instability, which has to scale with the size of the bump, can be predicted to be (6)

$$\Lambda \sim 25\, L$$

where $L = h_0 (3\eta V/\gamma)^{-1/3}$ is the length over which the capillary term (curvature term) is comparable to the Marangoni velocity. No calculations including gravity are available yet.

2. Non-hydrodynamic effects

At the edge of the film, disjoining pressure terms might well play a role. It is easy to get at least some idea of their importance from the analysis proposed by de Gennes (8). Let θ be the dynamic contact angle at the edge (θ can be defined for thicknesses in the micrometer range) before the crossover to the thin wetting film (fig.6).

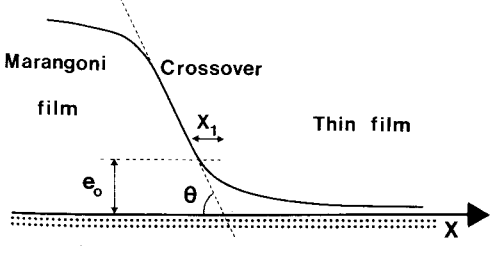

Fig.6 Transition from thick (Marangoni) to thin film and associated parameters.

The thickness e_0 at the crossover and the crossover length x_1, depend on θ. Roughly, $e_0 \approx a/\theta$ and $x_1 \approx a/\theta^2$ where a is a molecular size. Let us take a $\sim$ 1nm and use the measured θ values to calculate e_0 and x_1 (the diameter of the squalane molecule in L.L. experiments is $\sim$ 9 Å).

The results can be found in table I. Clearly, the thin film plays little role in our experiment, except for the smallest gradient. On the contrary, it must not be ignored in the L.L. experiment. This can be seen also by comparing the measured values of θ with the ones calculated from velocity and the hydrodynamic Tanner law (9):

$$\theta_T \approx 3.6 \left(\frac{\eta V}{\gamma}\right)^{1/3}$$

Systematic discrepancies occur in L.L. experiment, which again suggests that disjoining pressure terms have to be included in the dynamic equations.

(Let us note that the preceding discussion is largely qualitative: the formulae for x_1 and e_0 have been established in the case where $\theta = \theta_T$. A further analysis would be needed in the case where the apparent contact angle itself is changed due to the presence of the film. Strictly speaking, the"contact angle" is not defined any more).

III. Comparison with experiments - Discussion

1. Experimental results

The measured values of the velocity before fingering (V_{exp}) and the fingering wavelength Λ in our experiment are reported in table II and compared with the predicted ones. The agreement is satisfactory for the velocities and also for the ratio Λ/L (average measured value 20, calculated value 25).

Unfortunately, no theory is available yet for the developed

TABLE II

η (mPa.s)	τ (Pa)	h_o (μm)	v_{exp} (μm/s)	Λ (μm)	v_{th} (μm/s)	L (μm)	$\frac{\Lambda}{L}$
20	0.5	0.86	8	600	10.7	27	22
20	0.27	0.65	3	610	2.8	27	22
20	0.21	0.54	3	480	2.8	25	19
20	0.10	0.27	1	370	0.68	20	18
20	0.054	0.17	0.3	340	0.23	18	19
100	0.21	0.65	0.8	580	0.7	28	21
500	0.21	0.33	0.1**	340	0.07	18	19

** : linear part not clearly defined (smoothly varying slope).

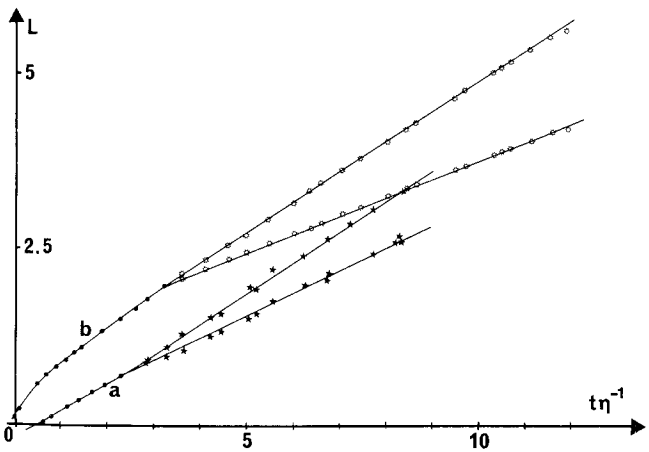

Fig.7 Length of the Marangoni film as a function of t/η.
Upper curve : $\tau = 0.21$ Pa $\eta = 0.1$ Pa.s .
Lower curve : $\tau = 0.21$ Pa $\eta = 0.02$ Pa.s.
For each curve the upper line corresponds to the position of the "hills", the lower line to the position of the "valleys".

instability, although it is certainly governed by simple laws, at least to a certain extent: fig.7 shows that both hills and valleys climb with constant velocities, U_{max} and U_{min} respectively. There is also evidence that the finger profiles scale with h_0 and depend on the ratio U_{max}/U_{min} (10).

No theory is available either for describing the injection condition in our system and predict the value of h_0.

In the L.L. experiment, the agreement between the measured and calculated velocities is also very satisfactory.

2. Discussion

The climbing rate of wetting films driven by temperature-induced surface tension gradients is well accounted for by hydrodynamic equations.

It is not so for the film profile and for the fingering instability which takes place for non-monotonous profiles with bumps. The origin of the bump is only partly understood: that V_F must increase with h_0 is clear, but the role of the precursor film - which tends to smooth out the profile and reduce the bump - has still to be analysed. Also the crossover regime between film with or without bump, and the existence of an instability threshold (does it coincide with the occurrence of the bump ?) must be investigated.

Acknowledgments : Fruitful discussions with M. Cazabat and P. Levinson are gratefully acknowledged.
This work has been partly supported by a D.R.E.T. grant.

Literature

[1] Heslot F., Cazabat A.M., Fraysse N. (1989): in "Liquids - J. Phys. D". 1, 5793 (1989).

[2] B.V. Deryaguin, N.V. Churaev : J. Colloid Interface Sci. 54, 157 (1976).

[3] A.M. Cazabat, F. Heslot, S.M. Troian and P. Carles : Nature, 346, 824 (1990).

[4] V. Ludvikson and E.N. Lightfoot : AICHE Journal 17, 166-1173 (1971).

[5] Heslot F., Cazabat A.M., Levinson P.: Phys. Rev. Lett. 62, 1286 (1989).

[6] E. Herbolzheimer and S.M. Troian : to appear.

[7] P. Carles : unpublished results.

[8] de Gennes P.G. : Rev. Mod. Physics 57, 828 (1985).

[9] L.H. Tanner : J.Phys. D 12, 470 (1983).

[10] A.M. Cazabat, F. Heslot : Colloids and surfaces 51, 309 (1990).